Precipitation Retrieval from Spaceborne Microwave Radiometers Based on Maximum *a posteriori* Probability Estimation

Nazzareno Pierdicca, Frank Silvio Marzano, Giovanni d'Auria, Patrizia Basili, Piero Ciotti, *Member, IEEE,* and Alberto Mugnai

***Abstract*— A retrieval technique for estimating rainfall rate and precipitating cloud parameters from spaceborne multifrequency microwave radiometers is described. The algorithm is based on the maximum *a posteriori* probability criterion (MAP) applied to a simulated data base of cloud structures and related upward brightness temperatures. The cloud data base is randomly generated by imposing the mean values, the variances, and the correlations among the hydrometeor contents at each layer of the cloud vertical structure, derived from the outputs of a time-dependent microphysical cloud model. The simulated upward brightness temperatures are computed by applying a plane-parallel radiative transfer scheme. Given a multifrequency brightness temperature measurement, the MAP criterion is used to select the most probable cloud structure within the *cloud-radiation data base.* The algorithm is computationally efficient and has been numerically tested and compared against other methods. Its potential to retrieve rainfall over land has been explored by means of Special Sensor Microwave/Imager measurements for a rainfall event over Central Italy. The comparison of estimated rain rates with available raingauge measurements is also shown.**

I. Introduction

RAINFALL RATE estimation by means of microwave radiometric measurements from space has been long considered an appealing goal [1], [2]. The increasing interest into precipitation estimates is due both to the emerging needs of global climate change modeling and to the impact of rain on human activities [3].

The physical foundations of precipitation retrieval using space borne microwave radiometers are based on the fact that the upwelling brightness temperatures from the atmosphere are influenced in a frequency dependent way by the vertical profiles of meteorological parameters, namely by the vertical distributions of various hydrometeors which are present in clouds, and by the Earth's surface characteristics [4]. The direct problem of finding the upwelling brightness temperatures, once all the parameters are known, has found satisfactory solutions at least for simple geometry of clouds. The solutions are based on the radiative transfer theory in presence of albedo and various methods have been successfully implemented [5]–[7]. However, the inverse problem of finding one or more physical parameters (rain for instance) from the knowledge of upwelling brightness temperatures at various suitable frequency channels has so far found great objective difficulties. This is mainly due to the great number of parameters which compete with the required one in determining the radiometric measurements.

There are at least two main aspects which become of importance when the retrieval process is attempted: 1) the use of an appropriate data base of the physical parameters of the atmosphere, and namely of the clouds, to act as input to the radiative transfer model; and 2) the choice of decision criteria for assigning the "best" value to the retrieved parameters of clouds (i.e., the retrieval algorithm). As far as the data base is concerned, the possibility to acquire data from specific experiments either *in situ* or by means of radars is scarce, especially considering the detailed information required for vertical profile retrieval. Rainfall can be measured fairly easily at the surface, but difficulties are still occurring in large areas. Some authors have assumed the vertical distributions of hydrometeors and other parameters according to climatological and physical considerations. Climatological models for temperature and water vapor profiles can be provided. Clouds, for instance, can be thought vertically divided in three or four fundamental layers where water exists only in the liquid state, or in the solid state or in a mixture of the two states [8], [9]. These assumptions can account for the mean values of the parameter profiles (climatological profiles), but to take into account the stochastic nature of the atmospheric variables, other hypotheses are needed regarding the random fluctuations of the variables around their means. Other authors have used microphysical models of evolving storms to establish data bases [9]–[11]. In this case, one has to admit that these models, while describing the evolution of a precipitating cloud, account for a large variety of cloud types. An advantage of data bases derived from the microphysical models is that they can furnish intrinsically the random fluctuations of the profiles besides their mean value. The statistical parameters of these fluctuations are physically consistent and so are the correlations among hydrometeors [12], [13].

Manuscript received August 15, 1995; accepted March 1, 1996. This work was supported in part by the Italian Space Agency (ASI), the Ministry of University and Research (MURST), the European Union (EU), and the Gruppo Nazionale per la Difesa dalle Catastrofi Idrogeologiche (GNDCI). The SSM/I data were provided within NASA's WetNet Project.

N. Pierdicca, F. Silvio Marzano, and G. d'Auria are with the Department of Electronic Engineering, University "La Sapienza," Rome, Italy.

P. Basili is with the Institute of Electronics, University of Perugia, Italy.

P. Ciotti is with the Department of Electrical Engineering, University of L'Aquila, Italy.

A. Mugnai is with the Institute of Atmospheric Physics, National Research Council, Rome, Italy.

Publisher Item Identifier S 0196-2892(96)05056-5.

Regarding the adopted procedures to retrieve cloud parameters, it is noted that almost all are of statistical nature, although this aspect is not always put in a consistent statistical framework. This fact emphasizes the need of a data base which is physically and statistically representative in order to work out the retrieval process. To put it simply, the retrieval procedure has to choose from the data base the cloud structure which is consistent with the microwave radiometric signature of the cloud (i.e., the measurements) or, in other words, the cloud structure which gives upwelling brightness temperatures which "resemble" those furnished by the measurements. This concept can be expressed analytically in a number of ways, although the intrigued set of assumptions often made leads in most cases to results which do not differ substantially from each other. Some considerations are necessary, however. First, the data base must be large enough in order to properly define the statistics of the cloud structure and account for various typologies of clouds. Second, ambiguities can occur for the nonuniqueness of the solution of the inverse problem (a suitable choice of the radiometric channels is required). Finally, errors are always present for inadequateness of models and noise of the instruments and they can be magnified during the retrieval process. The latter two considerations are common to almost all inversion problems [14] and the various algorithms try to overcome these difficulties [15]. The first consideration may lead to a large computing time and methods to partially remove such a problem can be envisaged. One way is an iterative perturbation approach to enlarge the information originally contained in the data base [8], [16].

Among the various algorithms appeared in literature for retrieving precipitation and other cloud parameters, the most used approach is based on the minimization of the mean squared departure (sometimes weighted) of the solution of the radiative transfer model from the measurements. However, this solution is not linearly related to the physical variables of the cloud and, in general, an analytical expression of the estimated parameters cannot be given. Some authors nevertheless have used a linearization of the solution either in the entire set of the realizations (the data base) or in a subset of these [10], [12], [17]. Least mean squared error approaches, with linearization assumptions, are in the framework of the regression theory and results have been presented both for simulated and experimental data. To overcome the linearization assumptions, nonlinear fitting or piece-wise approximations have been used [8], [18], [19]. Furthermore, considering the opportunity of retrieving more cloud parameters and not only surface rain rate, multiple multivariate regressions have been also used [13]. Other approaches explicity use a minimum Euclidean distance between the measured temperatures and the simulated ones [8], [16], [19], [20]; or criteria based on the statistical theory of parameter estimation [21], [22]. Results may be similar to the other approaches, according to the way for which errors are accounted.

In this paper, we present a comprehensive approach aiming at the estimation of precipitating cloud parameters from multifrequency radiometric measurements. It can represent an intermediate procedure with respect to those so far adopted. The primary data base we have used is derived from a microphysical model of an evolving storm, but it is further expanded by means of the random addition of Gaussian-distributed perturbations while maintaining the same mean parameter values and covariance matrix. The procedure allows one to integrate different sources of information (models, radar data, etc.) and to reasonably modify the statistical parameters to extend the data base to other classes of clouds. The retrieval algorithm is presented in the framework of the statistical theory of parameter estimation and aims at the evaluation of the entire cloud vertical structure rather than surface rain rate only. It does not imply any linear relationship between measured brightness temperatures and cloud parameters, takes into account the possible sources of errors and does not require large computer resources.

Section II presents an overview of the entire procedure by singling out the main functions and data flows. Each step of the process of generating a data base of cloud structures and related brightness temperatures (the *cloud-radiation data base*) is further detailed in Section III. In order to give to the reader a better insight into the meaning and the limitations of the proposed method, an assessment of the characteristics of the data base is presented in Section IV. Details about the retrieval algorithm and a test of the algorithm on simulated data are presented in Section V. The simulations have been performed considering the same set of frequency channels (19.3, 22.2, 37.0, and 85.5 GHz) used by the Special Sensor Microwave/Imager (SSM/I) on board the DMSP satellite [23]. Finally, the method has been applied to SSM/I data acquired in the Mediterranean area during a significant precipitation event. In Section VI the retrieved rain rate map is compared to raingauge measurements available in the precipitation area.

II. Overview of the Retrieval Method

The entire procedure for retrieving cloud parameters and rain rate is illustrated in the block diagram of Fig. 1, where rectangular boxes stand for procedures and oval ones indicate data bases. The direct problem is shown on the right hand side by white boxes, while the gray boxes show the various steps for arriving at the estimation of the cloud parameters (inverse problem). The various steps involved are briefly explained below. Further details are given in the following paragraphs.

1) Primary Cloud Data Base: Here we refer to a cloud data base derived from a microphysical model of an evolving storm, but other sources of information can be envisaged, such as radars, local soundings, etc. This data base gives in a three-dimensional space grid the equivalent water contents (EWC) of four hydrometeor species (rain drops, cloud droplets, graupels, and ice crystals and aggregates) and the values of pressure, temperature, and water vapor content.

2) Statistical Sampling: The cloud data are transformed in a statistical, one-dimensional data base (the *processed cloud data base*). The four hydrometeor EWC's, pressure, temperature, and water vapor at each altitude, but at different times and horizontal locations are all considered as possible realizations of the cloud, and their fluctuations of values furnish the statistical nature of the cloud data base.

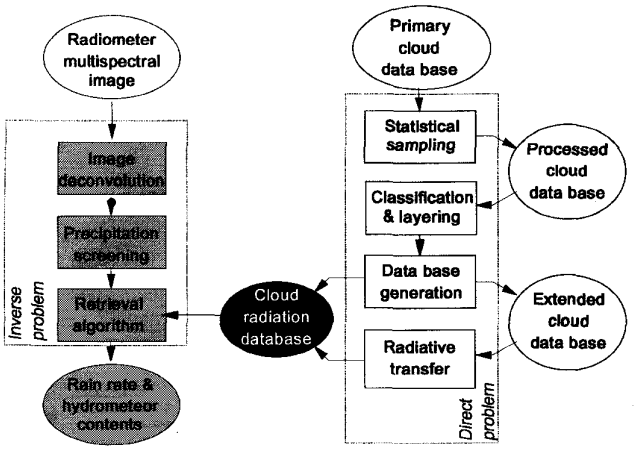

Fig. 1. Overview of the retrieval method. Functions and data flow.

3) Classification and Layering: The *processed cloud data base* contains diverse typologies of cloud because it has been composed gathering together cloud structures in different parts and at different times of an evolving storm. In fact a number of classes or cloud types can be defined and a statistical analysis of each class can be carried out in order to find, at each considered vertical level, the mean values of the hydrometeor EWC's and the covariance matrix relative to the four hydrometeor EWC's at different vertical levels. To make more manageable these statistical results, a reduction of the vertical levels is needed (layering procedure).

4) Data Base Generation: Only five classes of cloud have been considered, which in some way resemble those of a conventional meteorological classification. However, the retrieval algorithm requires a large amount of cloud data to work satisfactory. Therefore a new data base is generated by using random distributions of cloud parameters with the same mean vector and covariance matrix as the ones obtained by clustering (*extended data base*).

5) Radiative Transfer: This process completes the solution of the direct problem thus furnishing the *cloud-radiation data base* that includes both cloud data and related brightness temperatures. To solve the radiative transfer equation other parameters must be introduced in the model besides the hydrometeor EWC's, such as the radiative properties of the surface below, size distributions of particles, their phase functions and so on. The incompleteness of this information increases the error in the estimation process and should be taken into account.

6) Image Deconvolution: As far as the inverse procedure is concerned, we start from the images of the upwelling brightness temperatures measured by the multichannel satellite radiometer. In the following we have considered the four SSM/I channels at 19, 22, 37, and 85 GHz. However, the spatial resolution provided by the channels is not the same. For instance, the 85 GHz channel gives a resolution of 12 × 15 km, while the 19 GHz channel of 69 × 43 km. Therefore, in order to use a multifrequency retrieval algorithm, it is necessary to have the same resolution at all channels thus reducing the resolution of the highest channels and increasing the one of the lowest channels. The best effect can be accomplished by a deconvolution process which in part reduces the smearing effect of the antenna. However, this cannot be sufficient and a spatial averaging of the highest channels can be necessary. In this work we have used the Backus-Gilbert deconvolution technique developed by Farrar and Smith [24].

7) Precipitation Screening: It can be profitable to separate the nonrainy events from the set of measurements in order to apply the retrieval procedure only to the precipitation areas. This can be obtained in different ways. If the radiometer channels (or some of them) have two polarizations, we can exploit the polarization diversity induced by the surface below to distinguish a water surface from precipitation [25], [26]. Or yet we can use a double clustering approach operating on the principal components of the multispectral images [21].

8) Retrieval Algorithm: The retrieval algorithm is used to infer the hydrometeor profiles calculated for the seven layers. The surface rain rate is derived from a rainfall model [10]. The used retrieval algorithm is based on a probabilistic approach minimizing on average a cost function or specifically finding the cloud parameters which give the maximum *a posteriori* probability, as extensively explained in Section V.

III. Generation of the Cloud-Radiation Data Base

A. Statistical Sampling

The *primary cloud data base* we have used in this work was generated by a three-dimensional time-dependent cloud mesoscale model known as the University of Wisconsin-Nonhydrostatic Modeling System (UW-NMS) [27]. One of its main features is the presence of an explicit microphysics for describing the dynamics of different kinds of hydrometeors, specifically: nonprecipitating ice (crystals plus aggregates); precipitating ice (graupel particles); nonprecipitating liquid water (cloud droplets); and precipitating liquid water (rain drops). We have used the results of a four-hour simulation of an intense summer hailstorm that occurred near Eldridge, AL. The various hydrometeor profiles were sampled every one minute throughout the course of the simulation at an horizontal resolution of 1 km over a spatial extent of 50×50 km^2, and a vertical resolution of about 0.5 km (determining 42 altitude levels). The size distributions of each hydrometeor is a negative-exponential distribution with a given logarithmic slope (assigned for each hydrometeor category) and an intercept that is deduced from the hydrometeor content [10].

The output of the model has been processed to determine a statistical one-dimensional data base of clouds to be used in subsequent statistical analysis. At any height and time step, hydrometeor liquid water densities were horizontally averaged within 10 km horizontally homogeneous cloud boxes to simulate the spatial averaging of the SSM/I antenna at the highest frequency band [10]. In conclusion, 768 cloud structures were obtained, each one consisting of four profiles of the equivalent water contents of each hydrometeor and three profiles of the other meteorological quantities (air pressure, temperature and specific humidity), plus the value of the surface rain rate (RR). Each individual structure can be related

to different features of the storm during its time evolution and to different locations within the storm horizontal extension. We have intended that these 768 profiles may represent different realizations of a cloud belonging to a continental precipitation event.

B. Cloud Classification and Statistical Analysis

The classification task can be accomplished by using the cloud physical parameters (i.e., the various hydrometeor contents) or their radiative behavior (i.e., the upwelling brightness temperatures). In this paragraph we present the first approach, which allows a clear interpretation of each class in terms of standard meteorological classifications. However, we can proceed similarly by performing the classification on the basis of the multifrequency T_B and the results will be compared in Section IV-A.

For the sake of simplicity we have used the columnar values of the hydrometeor water contents (columnar equivalent water contents, hereafter CEWC) that have been processed by using a disjoint clustering analysis based on the Euclidean distances. The data base is divided into clusters (classes) such that every sample belongs to one and only one class. The *nearest centroid sorting* technique is used, where a set of CEWC values, called cluster seeds, is selected as a first guess for the cluster centroids. Each sample in the data base is assigned to the nearest seed to form temporary clusters using a criterion based on the Euclidian distance of CEWC values from the current centroid. The seeds are then replaced by the centroids of the obtained clusters and the process is repeated until no further changes occur in the clusters. We have selected a number of classes (N_c) equal to five, each of them containing a significant number of clouds as needed for subsequent statistical computations.

Fig. 2 shows two scatterplots between CEWC's of different hydrometeor species where classes are represented by using different symbols. The graupel CEWC is presented against the ice CEWC and the cloud CEWC against the rain CEWC. It is interesting to note that the adopted classification algorithm determines classes that can be related to different parts of the simulated storm and therefore can also represent different types of clouds. In particular class 2 can be associated to the rear anvil of the storm, class 3 to the first cell and classes 4 and 5 to the main core [10].

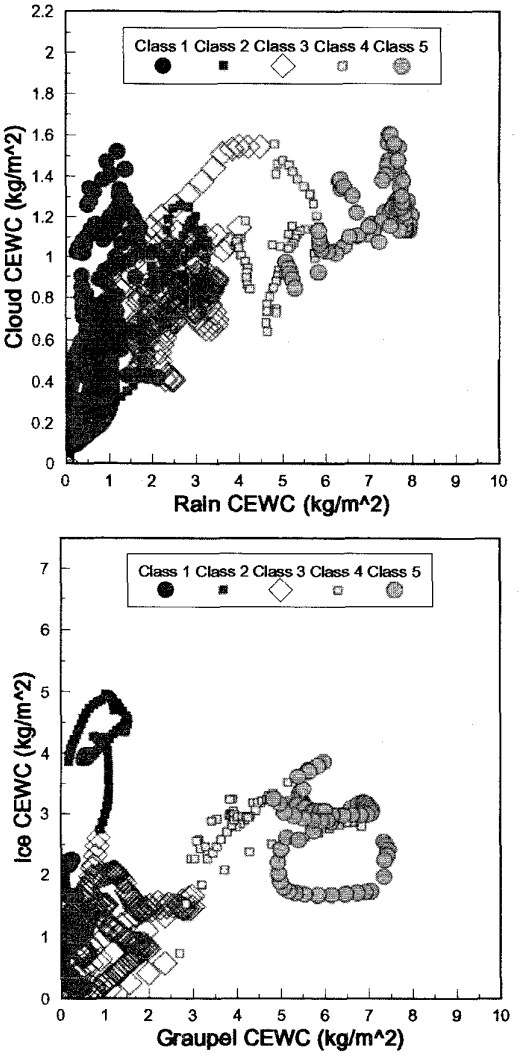

Fig. 2. Scatterplots of CEWC's of the processed data base (using the CEWC classification).

C. Layering Reduction Method

The method for reducing each cloud structure of the *processed cloud data base* to a limited number of layers consists of the following steps.

1) The 42-level EWC profiles provide the upper and lower boundaries of the four hydrometeors. The existence of any given hydrometeor has been assumed by defining a threshold level (10^{-4} kg/m^3). These boundaries define eight levels and therefore seven layers where different combinations of the hydrometeors are present.
2) The eight levels of each cloud structure have been averaged in each class in order to identify only one geometric configuration of seven layers.
3) Each 42-level cloud profile has been replaced by the corresponding 7-layer structure. In each layer an EWC corresponding to the average in its vertical extent has been assumed for each hydrometeor. As far as pressure, temperature and specific humidity are concerned, the mean profiles have been used for each class.

As a consequence, the *processed cloud data base* is reduced to a series of cloud structures with at most seven layers. The geometry, the pressure, temperature and humidity, as well the occurrence of each hydrometeor species in the layers are characteristic of the class. The cloud realizations are therefore identified by at most 7×4 values of EWC's for a total of 28 variates that will be considered the elements of a random vector $\boldsymbol{g}$. It must be pointed out that layers do not always contain all the hydrometeor species and therefore 28 is only an upper limit. As an example, Fig. 3 shows the class mean profiles of hydrometeor equivalent water densities obtained for a class with a medium-high value of ice and graupel content

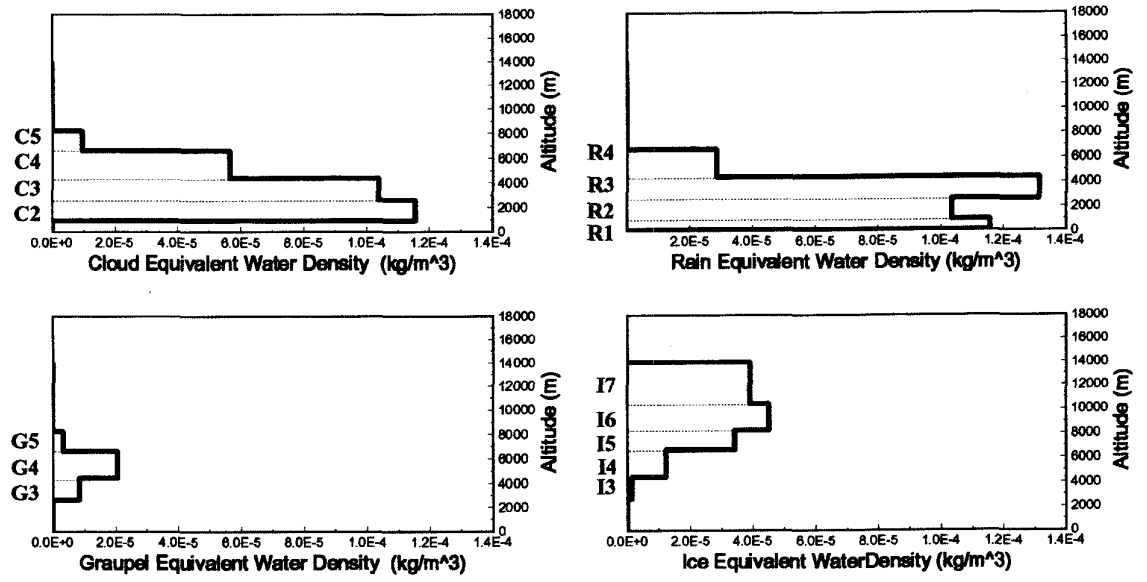

Fig. 3. Mean vertical profiles of equivalent water densities (kg/m^3) of different hydrometeor species for a class with a medium-high content of ice. In the left vertical axes the initial of the hydrometeor name is followed by a number which identifies the layer (increasing from the surface to the top of the troposphere).

(class 4); in this particular case, the procedure has resulted in cloud structures defined by 15 EWC values plus rain rate for a total of 16 variates.

D. Random Generation of Cloud Data Bases

As explained before, each cloud is defined by a vector $\boldsymbol{g}$ of dimension $D \times 1$, whose elements are at most the 28 geophysical parameters (the hydrometeor EWC's). For each class of the *processed cloud data base,* we have adopted a truncated Gaussian multidimensional joint-distribution of vector g, that is derived by setting to zero negative values of a Gaussian random vector whose probability density function (pdf) is given by the following equation:

$$p(\boldsymbol{g}) = \frac{1}{(2\pi)^{D/2}\sqrt{\det(\boldsymbol{C}_g)}} \exp\left[-\frac{1}{2}(\boldsymbol{g}-\boldsymbol{m})^T \boldsymbol{C}_g^{-1}(\boldsymbol{g}-\boldsymbol{m})\right] \tag{1}$$

where $\boldsymbol{C}_g$ $(D \times D)$ and $\boldsymbol{m}$ $(D \times 1)$ are the covariance matrix and the mean vector of $\boldsymbol{g}$; and $\det(\ )$, superscript $(\ )^{-1}$ and superscript $(\ )^T$ indicate the determinant, the inverse matrix and the transposed matrix operators, respectively.

This choice comes from the consideration that vector g is always positive and, especially for optically thin clouds with layers where the hydrometeor contents are small, can present zero values also, thus making questionable the assumption of alternative distributions like the log-normal one. Computations of the hystograms of the hydrometeor contents in the *processed data base* and hypothesis tests for the marginal pdf of each parameter have shown the adequateness of the choice. However, the required truncation does occur only in a very limited number of cases and its effect will be neglected in the calculation.

For each class we have generated new realizations of the geophysical vector $\boldsymbol{g}$ according to a Gaussian distribution with mean vector and covariance matrix already calculated for that class. We have used the so-called *rejection* technique described in [28]. Using this technique, a new extended cloud data base has been generated, consisting of 1000 structures for each class, that is a total set of 5000 structures has become available. Indeed, the number of generated clouds may be only limited by the computational efficiency required when running the retrieval procedure.

Fig. 4 presents the results in terms of the hydrometeor CEWC's of the randomly generated clouds. When comparing these scatterplots to those of Fig. 2, it can be noted that the number of points is largely increased even in regions where the original data appear very sparse; however, the fundamental correlations within the cloud structures originating by the microphysical model have been retained. In Section IV we will assess the capability of this data base to determine a swarm of points, in the domain of multifrequency brightness temperatures, dense enough compared to the radiometer sensitivity and the requirements of the retrieval algorithm.

E. Radiative Transfer Model

The radiative transfer model assumes a plane-parallel geometry for the precipitating clouds so that the effects of the cloud geometry in the horizontal dimensions have not been taken into consideration. This assumption is justified when the precipitating cloud is horizontally homogeneous within the field of view of the space-borne radiometer. The scalar radiative transfer equation in the microwave spectrum applies to the considered azimuthally symmetric structures and can be expressed as follows:

$$\frac{dT_B(\mu,\tau)}{d\tau} + T_B(\mu,\tau) - \frac{1}{2}\int_{-1}^{1} p(\mu,\mu',\tau)T_B(\mu',\tau)\,d\mu' = [1-w(\tau)]T(\tau) \tag{2}$$

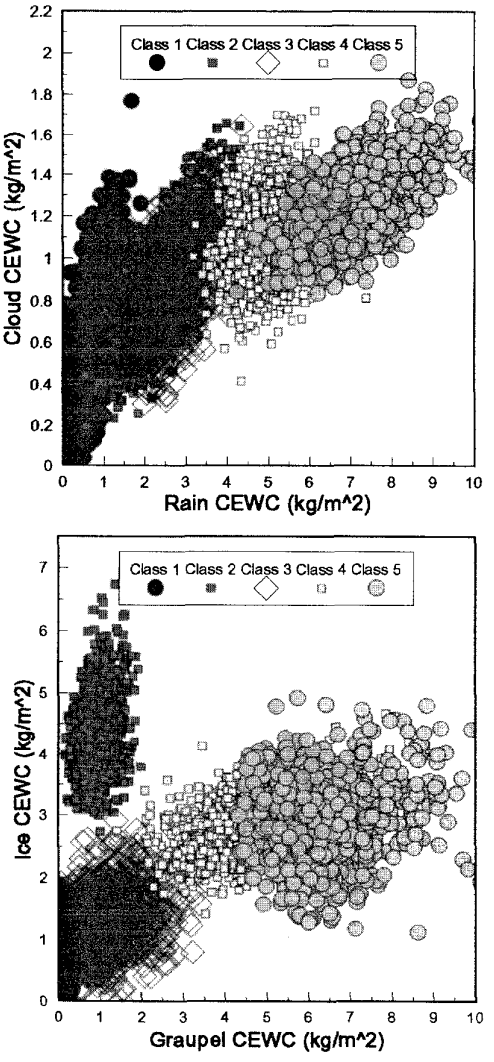

Fig. 4. Scatterplots of CEWC's of the randomly generated cloud data base (using the CEWC classification).

where T_B is the azimuthally independent brightness temperature in the direction θ with respect to vertical axis (being $\mu = \cos\theta$), τ is the vertical optical thickness from a given altitude to the top of the atmosphere, w is the single-scattering albedo, T is the physical temperature, and p is the azimuthally-averaged phase function. We have applied the method of discrete-ordinate for solving the integro-differential equation (2) [6], [7].

All the hydrometeors are supposed to be spherical so that Mie theory has been used to compute the single-scattering quantities; nonsphericity effects on polarized radiative transfer computations have not been considered. The refractive index of water hydrometeors is calculated from the drop temperature by means of the Ray approximation of Debye's formula, the ice refractivity by using an empirical formula, while the graupel refractivity has been derived by assuming the Maxwell–Garnet mixing formula [10]. The single scattering quantities in each layer have been obtained by summing the contributions of all hydrometeors; each contribution has been derived by averaging the scattering quantities over the drop-size distributions assumed in the mesoscale microphysical model. All the hydrometeors are embedded in a specified atmosphere, where pressure, temperature and water vapor vertical profiles are given, so that the gaseous absorption has been calculated using the Liebe model [29]. The Heyney–Greenstein phase function is assumed, which is specified by the mean asymmetry factor of the hydrometeors in the layer and corrected for high asymmetric forward scattering [30].

The Earth's surface has been considered a Lambertian surface whose emissivity is determined on the basis of simple models available from the literature [31]. The results reported in this paper have been obtained by considering a land characterized by a surface temperature of 25°C and moist factor of 0.9, that corresponds to a surface emissivity of about 0.85 for all the considered frequencies.

The output of the radiative transfer model allows one to associate to each cloud structure described by vector $\boldsymbol{g}$, a vector $\boldsymbol{t}$ whose elements are the upwelling brightness temperatures at the various frequencies and therefore to build the so called *cloud-radiation data base*. At this stage of the process, modifications of the class data bases can be accomplished to make the simulated microwave signatures to adhere more closely to radiometric measurements of actual cloud structures.

It must be pointed out that there are several approximations in the radiative transfer model we have applied and in the way the convolution of the antenna is taken into account. In particular, the kind of convective cloud model simulations we have utilized does not yield necessarily horizontally homogeneous fields on the scale of 10 km. Therefore, one should use a three-dimensional radiative model which accounts for the off-nadir observation angle of the radiometer [33]. Methods to consider a one-dimensional radiative transfer, including the approach we have proposed here, may lead to errors of several degrees. Moreover, the hydrometeor size distributions play a crucial role in the radiative transfer computation. In this work we have considered size distributions according to what is assumed in the cloud microphysical model, but alternative distributions are also under consideration [32].

IV. Analysis of the Cloud-Radiation Data Base

Some analyses of the derived *cloud-radiation data base* are significant for understanding its potential and they are reported in the following sections.

A. Comparison of Diverse Classifications

The classification algorithm applied either to the CEWC or to the T_B values groups the clouds in different ways. Considering the same number of classes ($N_c = 5$), Table I shows a 5×5 confusion matrix containing the number of clouds assigned to class i by one classification, but placed in class j using the other classification. It has been already mentioned that the CEWC classification allows one to clearly identify classes of clouds related to a specific time or space location within the microphysical simulation output. It appears evident from Table I that the similarity among clouds as sensed

TABLE I
COMPARISON OF CLASSIFICATIONS OF THE PROCESSED CLOUD DATA BASE, BASED EITHER ON CEWC OR ON BRIGHTNESS TEMPERATURE (T_B) VALUES

					Classification on CEWCs	
	Class 1	**Class 2**	**Class 3**	**Class 4**	**Class 5**	**Total**
Class 1	256					256
Class 2	116	17	62			195
Class 3	5	62	101	1		169
Class 4			20	35	24	79
Class 5				22	47	69
Total	377	79	183	58	71	768
Classification on T_B values						

by the radiometer does not necessarily leads to the same physical interpretation; however, the classification based on T_B gives better results in terms of retrieval accuracy [13].

B. Effects of the Layering Reduction

In order to evaluate the effect of the layering reduction procedure on T_B computations, we have analyzed the difference between brightness temperatures resulting from the original 41-layer and those emerging from the corresponding simplified 7-layer structures. Fig. 5 shows the differences at the various frequencies by a scatterplot representation. These differences do not present any significant bias at all frequencies (the averaged differences are within ± 1 K). However, the 7-layer structures lead to an overestimation of the brightness temperatures of clouds with significant albedo and to a minor underestimation of clouds of lower albedo, at all frequencies. For the more tenuous clouds, the 7-layer structure tends to overestimate T_B and the errors become significant at the lower frequencies. The root mean square error due to layering is of the order of 3–5 K at all frequencies. We have also investigated the effect of each hydrometeor species on these differences and found that high values of ice and graupel CEWC's strongly affect the performance of the layering reduction procedure at the highest frequencies.

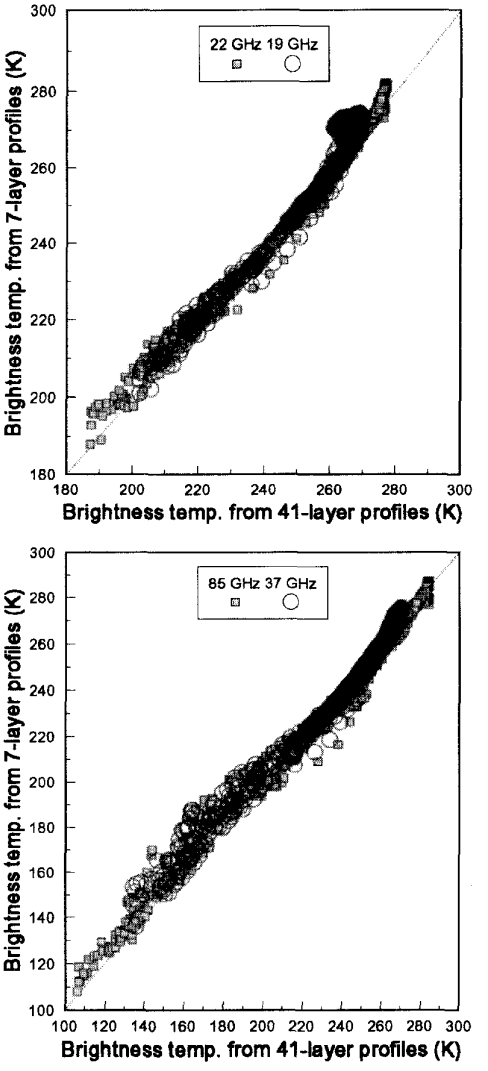

Fig. 5. Scatterplot of brightness temperature (T_B) values computed from the 41-layer and 7-layer clouds of the *processed cloud data base*.

C. Test of Density of the Cloud-Radiation Data Base

It is interesting to compare the radiometric behavior of the 5000 statistically generated cloud structures to that of the 768 structures of the *processed cloud data base*. Figs. 6 and 7 show, respectively, scatterplots between T_B values of different frequencies resulting from the original cloud structures and from those generated statistically. Top panels of each figure present T_B at 22 GHz versus T_B at 19 GHz, while bottom panels show the 85 and 37 GHz channels; each data point is represented by a different symbol, depending on the class it belongs to (T_B classification is considered in this case). As already discussed with reference to Figs. 2 and 4, it appears from these figures that the *cloud-radiation data base* reflects the radiometric signature of the *processed cloud data base*.

It is significant to quantify the density of points belonging to a certain data base. For this purpose, we have computed the Euclidean distance of each brightness temperature vector $\boldsymbol{t}$ to the closest one and defined the "density" of a data base as the distance below which 90% of the points occurs. It results that this distance for the *extended cloud data base* is of the order of 0.5 K that is comparable to the radiometric resolution of the current spaceborne radiometers and lower than the one of the *processed cloud data base* (about 2.5 K).

D. Brightness Temperature Sensitivity to Cloud Parameters

Since we are interested into hydrometeor vertical profile retrieval, we have analyzed the sensitivity of T_B to the variations of values of the hydrometeor EWC and other parameters of the radiative transfer (e.g., surface emissivity). For this purpose we have computed the T_B related to the mean cloud $\boldsymbol{m}$ and its variation ΔT_B when changing the elements of $\boldsymbol{m}$ and the surface emissivity one at a time. Fig. 8 shows ΔT_B for each layer of class 4 computed assuming variations of each cloud parameter equal to plus and minus one standard deviation, while the surface emissivity is varied according to what indicated in the figure (bottom-right panel). The T_B values at high frequencies (37 and 85.5 GHz) are very sensitive

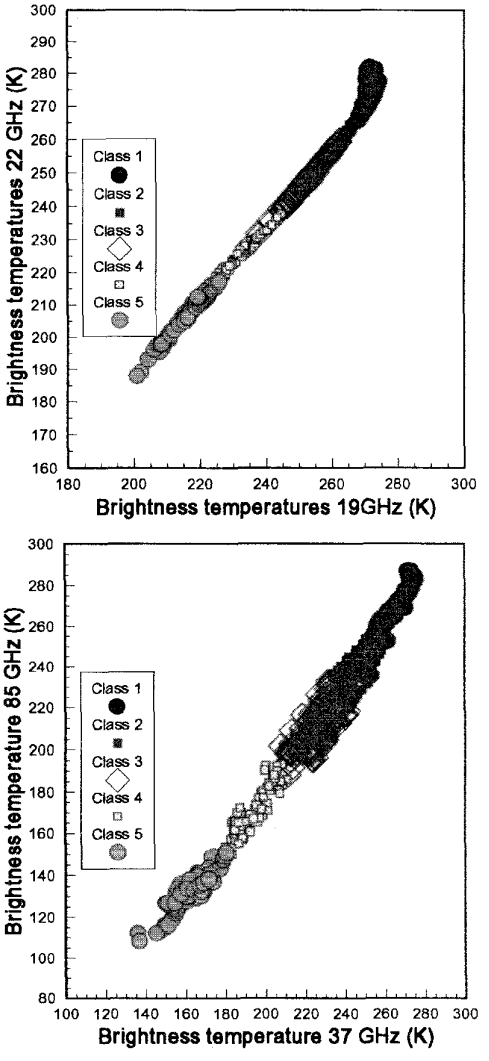

Fig. 6. Scatterplots of brightness temperature (T_B) values of the *processed cloud data base* (using the T_B classification).

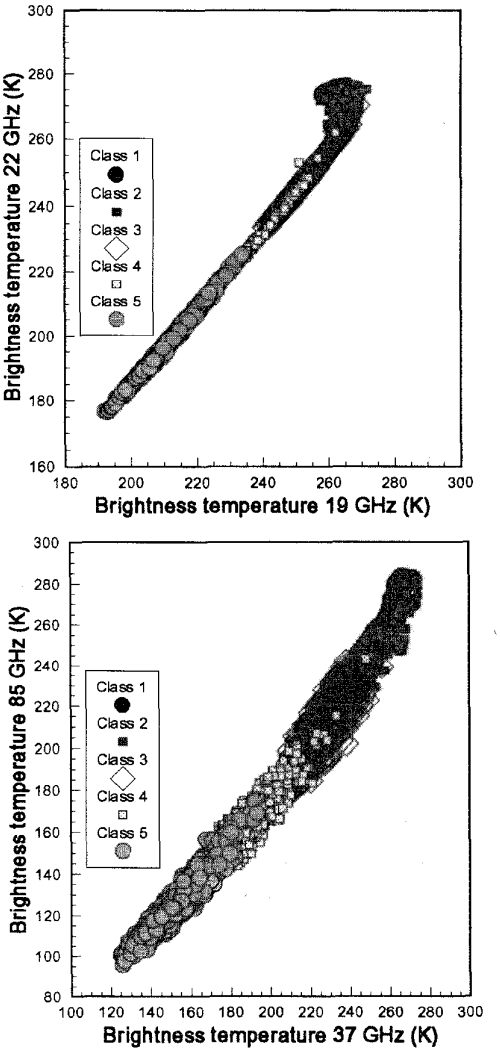

Fig. 7. Scatterplots of brightness temperature (T_B) values of the *extended cloud data base* (using the T_B classification).

to variations of the graupel EWC's in the highest cloud layers, while they are basically not affected by the variations of rain EWC's. On the contrary, the lowest frequencies are sensitive to the variation of the rain EWC of the middle layer (layer 3) and to the surface emissivity.

V. Retrieval of Hydrometeor Contents and Rain Rate

It has been observed that upwelling T_B at frequencies greater than about 19 GHz are almost not dependent on the structure of the lower rain layers and that the variability in the upper part of the cloud causes a large dispersion of the observed T_B against the rainfall rate. These considerations suggested that we retrieve at least a coarse vertical profile of the cloud parameters, thus exploiting the hydrometeor correlations at different altitudes and therefore improving the retrievals in the lowest layers. The rain rate, as well as other quantities of interest (e.g., latent heat) can be, therefore, computed from the retrieved vertical structure by means of a proper model. The model we have used to evaluate the rain rate is consistent with the UW-NMS microphysical model and is described in [10]. Briefly, the rain rate is obtained from an approximated expression of the mean flux of the precipitating water close to the surface, averaged over the drop size distribution.

As compared to other methods inferring the complete structure of the cloud, our algorithm searches the cloud profile within a *cloud-radiation data base* and therefore it exhibits fairly good performances in terms of processing time. The time consuming task of solving the radiative transfer equation is accomplished only once, when generating the *cloud-radiation data base*.

The retrieval algorithm has been tested on simulated data and compared to the results obtained by other well established methods, namely the multivariate linear regression and the algorithm which search for the cloud having the brightness temperature vector closest to the measured one (the minimum distance algorithm). The comparisons have been made mainly

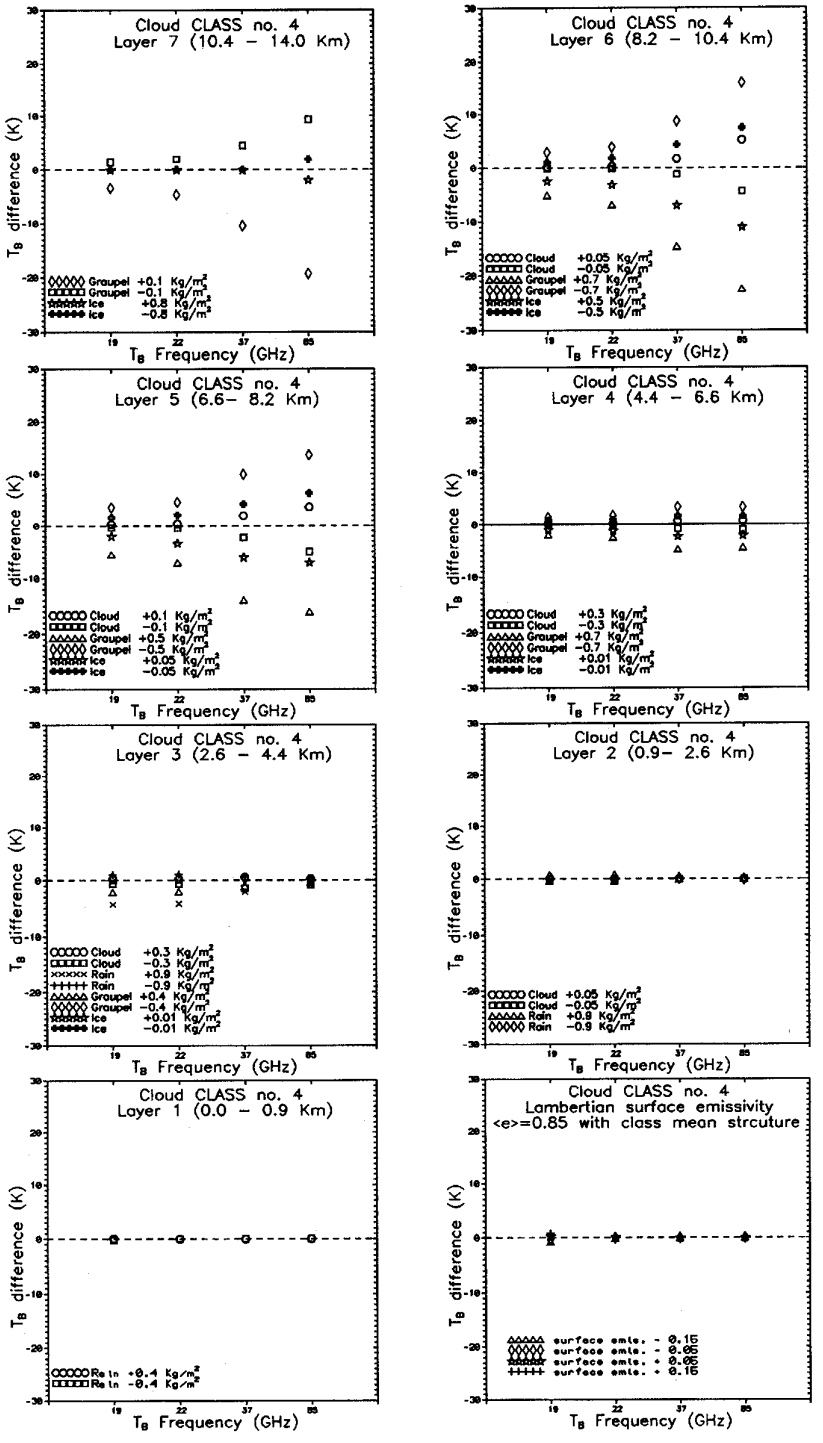

Fig. 8. Brightness temperature sensitivity to hydrometeor EWC's and surface emissivity for a class with a medium-high content of ice.

in terms of rain rate, but estimation of other cloud parameters have also been assessed. It should be mentioned that regression techniques are not only well established references to assess the improvements in accuracy using the proposed retrieval method, but still remain suitable for generating fast delivery and fairly robust products.

It must be noted at this stage that the statistical expansion of the data base does not really extend the microphysical settings of the cloud model to capture the many different actual clouds, but it is, however, necessary in order to run the retrieval algorithm with enough resolution of both geophysical parameters and brightness temperatures. As far as

future developments are concerned and in view of operational processing of radiometric data on a global scale, it will become necessary to concatenate the results from several different cloud model runs and therefore to include more and more classes of precipitation events in the *cloud-radiation data base.* To this aim we can also use radar data or, when necessary, we can slightly change some statistical parameters of the cloud classes, e.g., the values of the mean and variance vectors.

A. The Maximum a posteriori Probability Estimation

The hydrometeor vertical profile (identified by a vector $\boldsymbol{g}$) can be inferred from a multifrequency T_B measurement (expressed by vector $\boldsymbol{t}$) by applying the theory of parameter estimation which has been developed in the framework of signal detection and estimation. We can apply the maximum *a posteriori* probability criterion (MAP) that can be established within the more general Bayes estimation theory and is sometimes referred to as unconditional maximum likelihood criterion or maximum likelihood with *a priori* probability. If i is the discrete random variable that represents the ith class, we have to search for the cloud structure that maximizes the conditional pdf $p((\boldsymbol{g},i)|\boldsymbol{t})$ of a cloud structure $\boldsymbol{g}$ belonging to a class i, given a measure $\boldsymbol{t}$. Alternatively, by using the Bayes theorem, $p((\boldsymbol{g},i)|\boldsymbol{t})$ can be expressed in terms of the conditional pdf of a measurement $\boldsymbol{t}$, given a cloud structure $\boldsymbol{g}$ and a class i, that is

$$p((\boldsymbol{g},i)|\boldsymbol{t}) = \frac{p(\boldsymbol{t}|(\boldsymbol{g},i))p(\boldsymbol{g},i)}{p(\boldsymbol{t})}. \tag{3}$$

As already discussed in Section III-D, the pdf of the vector $\boldsymbol{g}$ belonging to a certain class i is assumed to be Gaussian. It should be noted that, within the above notation, (1) represents the pdf of a vector $\boldsymbol{g}$ conditioned to class i, i.e., $p(\boldsymbol{g}|i)$. Thus, the joint pdf of vector $\boldsymbol{g}$ and class i can be expressed as follows:

$$p(\boldsymbol{g},i) = \frac{1}{(2\pi)^{D/2}\sqrt{\det(\boldsymbol{C_{g_i}})}} \cdot \exp\left[-\frac{1}{2}(\boldsymbol{g}-\boldsymbol{m_i})^T\boldsymbol{C_{g_i}^{-1}}(\boldsymbol{g}-\boldsymbol{m_i})\right]P(i) \tag{4}$$

where $\boldsymbol{m_i}$ and $\boldsymbol{C_{gi}}$ are the mean vector and covariance matrix of the class i, respectively, and $P(i)$ is the probability of occurrence of the class (*a priori* probability), considering that the variable i is a discrete one.

The use of the Bayes theorem introduces the conditional probability $p(\boldsymbol{t}|(\boldsymbol{g},i))$ which represents the statistical distribution of T_B measurements for those cloud structures which we identify by the vector $\boldsymbol{g}$ and class i. The statistical fluctuations endured by vector $\boldsymbol{t}$ are due to various causes. We assume that those fluctuations or errors can be represented by an additive noise superimposed to the values $\bar{\boldsymbol{t}}$ of the brightness temperature vector determined by the adopted radiative model. Therefore, $\boldsymbol{t}-\bar{\boldsymbol{t}}$ represents the added random error whose probability distribution must be specified for applying the MAP procedure to (3). Such errors are caused by uncertainties determined by the modeling of the radiative transfer as well as instrumental noise. For instance, the former may be attributed to fluctuations of parameters not included in the adopted model (e.g., for the discretization of profiles through the layering reduction procedure), or even included, such as surface emissivity and numerical computation errors. Due to the many effects which causes the errors $\boldsymbol{t}-\bar{\boldsymbol{t}}$ and in order to simplify the procedure, we assume that such errors are normally distributed and have a zero mean value. To put in other words, the errors are assumed due to a large number of independent sources such that the central limit theorem can be applied. Therefore, the fluctuations of $\boldsymbol{t}$ occur around the value of $\bar{\boldsymbol{t}}$, determined from the model and correspondingly the conditioned pdf of $\boldsymbol{t}$ is

$$p(\boldsymbol{t}|(\boldsymbol{g},i)) = \frac{1}{(2\pi)^{D/2}\sqrt{\det(\boldsymbol{C_t})}} \cdot \exp\left[-\frac{1}{2}(\boldsymbol{t}-\bar{\boldsymbol{t}})^T\boldsymbol{C_t^{-1}}(\boldsymbol{t}-\bar{\boldsymbol{t}})\right] \tag{5}$$

where $\boldsymbol{C}_t$ is the covariance of the random vector $\boldsymbol{t}-\bar{\boldsymbol{t}}$, for the determination of which further assumptions are needed.

If we compute the natural logarithm of both members of (3), the maximization of $p((\boldsymbol{g},i)|\boldsymbol{t})$ requires to search for a cloud structure $\boldsymbol{g}$ and its associated class, that maximizes the following discriminant function $d(\boldsymbol{t},\boldsymbol{g})$:

$$d(\boldsymbol{t},\boldsymbol{g}) = \ln[p(\boldsymbol{t}|(\boldsymbol{g},i))] + \ln[p(\boldsymbol{g},i)] \tag{6}$$

where $p(\boldsymbol{t})$ has been removed as a common factor that does not contribute to discrimination, being equal for all the comparisons. If we substitute (4) and (5) and neglect the constant factor $-D/2\ \ln(2\pi)$, we find the following equation:

$$\begin{aligned} d(\boldsymbol{t},\boldsymbol{g}) = &-\tfrac{1}{2}\ln[\det(\boldsymbol{C_t})] - \tfrac{1}{2}(\boldsymbol{t}-\bar{\boldsymbol{t}})^T\boldsymbol{C_t^{-1}}(\boldsymbol{t}-\bar{\boldsymbol{t}}) \\ &- \tfrac{1}{2}\ln[\det(\boldsymbol{C_{g_i}})] - \tfrac{1}{2}(\boldsymbol{g}-\boldsymbol{m_i})^T\boldsymbol{C_{g_i}^{-1}}(\boldsymbol{g}-\boldsymbol{m_i}) \\ &+ \ln[P(i)]. \end{aligned} \tag{7}$$

As a further simplification, we assume that the components of the error $\boldsymbol{t}-\bar{\boldsymbol{t}}$ are uncorrelated at the different frequencies and have the same variance σ_t^2; consequently, the covariance $\boldsymbol{C_t}$ reduces to a diagonal matrix with diagonal elements equal to σ_t^2, and the term $\det(\boldsymbol{C_t})$ becomes a common factor that does not contribute to the discrimination. Thus, in the afore mentioned hypotheses, the MAP procedure requires the minimization of the following quadratic form:

$$\begin{aligned} &\frac{1}{2\sigma_t^2}(\boldsymbol{t}-\bar{\boldsymbol{t}})^T(\boldsymbol{t}-\bar{\boldsymbol{t}}) + \frac{1}{2}(\boldsymbol{g}-\boldsymbol{m_i})^T\boldsymbol{C_{g_i}^{-1}}(\boldsymbol{g}-\boldsymbol{m_i}) \\ &\quad + \frac{1}{2}\ln[\det(\boldsymbol{C_{g_i}})] - \ln[P(i)]. \end{aligned} \tag{8}$$

The first term represents the assumed squared errors and the second term a weighted square of the differences of the random vector $\boldsymbol{g}$ from its mean value, possibly interpreted as a climatological value or a first guess. In the above interpretation, the procedure closely resembles the regularization technique commonly used in statistical algorithms of inversion [14]. Moreover, the last two terms in (8) give a weight to each candidate $\boldsymbol{g}$, depending on the class it belongs to. It must be noted that no assumption of linearity is made for the relation between $\boldsymbol{g}$ and $\boldsymbol{t}$ and therefore no analytical expression for the

estimated $\boldsymbol{g}$ can be written. In the numerical implementation of the algorithm, the estimated cloud profiles is derived from the measured T_B values by querying the *cloud-radiation data base,* i.e., selecting the cloud structure $\boldsymbol{g}$ (and the associated $\bar{\boldsymbol{t}}$) that gives the maximum value of the discriminant function $d(\boldsymbol{t}, \boldsymbol{g})$ as compared to that calculated from all other available structures. Note that the size of the *cloud-radiation data base* has been chosen to ensure that a significant number of points have T_B values that fall within a radiometric noise of 1 K.

The hypothesis of assuming no correlation between errors in the diverse radiometric channels (i.e., $\boldsymbol{C}_t$ to be diagonal) is very severe, but we know only few sources of errors and a thorough investigation on matrix $\boldsymbol{C}_t$ would be hard to accomplish. The same is true for the choice of the value to assign to the variance σ_t^2. However, the role played by σ_t^2 in minimizing expression (11) appears to be rather a trade-off factor between the need of minimizing the errors and that of finding a value of $\boldsymbol{g}$ not too far from the mean. If a very small value is given to σ_t^2, the first term in (11) will prevail and we will choose $\boldsymbol{g}$ (i.e., a profile of the cloud structure) which produce $\bar{\boldsymbol{t}}$ nearest (in the Euclidean sense) to the measured brightness temperatures $\boldsymbol{t}$. We remind that from the adopted transfer model, points $\bar{\boldsymbol{t}}$ in the space of T_B are labeled in terms of $\boldsymbol{g}$. Vice versa, a large value of σ_t^2 forces the solution to coincide with the mean profile in the class having the highest *a priori* probability and smallest determinant of the covariance matrix.

The possibility to introduce the prior probability $P(i)$ of each cloud class is a relevant feature of this Bayesian estimator. However, at this stage of the work, we have not enough information to discuss on this because we are still working with a single cloud model simulation and we are analyzing specific precipitation events. This feature can be better exploited when the method is applied to operational processing of microwave radiometric data on a global scale. In this case, the prior probabilities of several classes of clouds included in the *cloud-radiation data base* may be related to the geographycal area and to the time of the observation.

B. Tests of the Algorithm on Simulated Data

The accuracy of the retrieval algorithm is estimated by computing the residual root mean square (rms) error between the retrieved parameter and the "true" value of it. In order to make a significant test of the retrieval procedure, the data set used to estimate the accuracy should be derived from a different set of cloudy events with respect to those used for running the algorithm (e.g., the *extended cloud data base*). We have approached this situation by deriving the set of radiometric measurements associated to known atmospheric situations and rain rates (the "true" atmosphere) from the 768 vectors $\boldsymbol{t}$ of the *processed cloud data base* (computed for the radiometric channels at 19, 22, 37, and 85 GHz). A zero mean uncorrelated Gaussian random error (with standard deviation of 1 K for all frequencies) has been added in order to account for instrumental noise. In this way we perform the test by using 41-layer cloud structures and therefore we account at least for additional errors due to the layering procedure.

As already mentioned in the previous paragraph, when applying the MAP criterion we have to make a choice about a plausible value of σ_t^2 that is assigned on the basis of the errors we know. While instrumental error is assumed 1 K, the error due to the limited number of layers in the model has to be properly taken into account. In particular, we have found that a minimum rms error on the estimation of the rain rate is obtained for a value of σ_t^2 nearly equal to 4, and this value has been assumed in the calculations.

By applying the MAP criterion to the simulated test data, we have retrieved the RR and the CEWC's of the different hydrometeor species. Assuming classes with the same *a priori* probability, we have found a residual rms of 4.6 mm/h for the rain rate, 0.28 $\mathrm{kg/m^2}$, 0.67 $\mathrm{kg/m^2}$, 0.26 $\mathrm{kg/m^2}$, and 0.86 $\mathrm{kg/m^2}$ for cloud, rain, graupel and ice CEWC's, respectively. The results are shown in the left panels of Fig. 9 where, as examples, the retrieved values of RR and graupel CEWC are plotted as function of the "true" values.

As far as the multivariate linear regression is concerned, the regression coefficients for estimating the parameters we are looking for (RR or hydrometeor CEWC's) are derived by using the *cloud-radiation data base* with a 1 K Gaussian random error added to the brightness temperatures to account for instrumental errors. With regard to the minimum distance algorithm, in our approach it simply represents a special case of the MAP algorithm, when only the Euclidian distance between brightness temperatures is considered in the discriminant function. The results of the linear regression and the minimum distance algorithms applied to the simulated test data are shown in the right panels of Fig. 9. The rms errors we have computed for the RR is 5.3 mm/h, both for the regression and the minimum distance algorithm, while for the graupel CEWC is 0.37 $\mathrm{kg/m^2}$ and 0.28 $\mathrm{kg/m^2}$, respectively.

VI. An SSM/I Case Study over Central Italy

This section presents a case study where the proposed retrieval method has been applied to SSM/I measurements over the Mediterranean area and compared to surface raingauge measurements to give indications about the potential of the method for retrieving precipitation from space. Another SSM/I application of the algorithm can be found in [21], while comparisons of the retrieval results with radar estimates are described in [19] and [32].

Fig. 10 shows images of the Mediterranean area acquired on November 24th, 1987 at 18:00 GMT by SSM/I. The figure provides an overview of the complete set of multifrequency T_B (22 GHz vertically polarized and 19, 37 and 85 GHz averaged on the two polarizations). The images are presented in the sensor coordinates so that distortions due to the scanning geometry are present. A uniform contrast stretching between 160 and 280 K and a common gray-scale have been applied, so that the patterns in the images can be directly interpreted in terms of temperature field patterns. A high contrast between land and sea appears in the lowest frequency channel (the top-left panel), while patterns related to the atmospheric contribution are more evident in the highest frequency channels (the right panels). In particular, the 85 GHz image makes it evident the

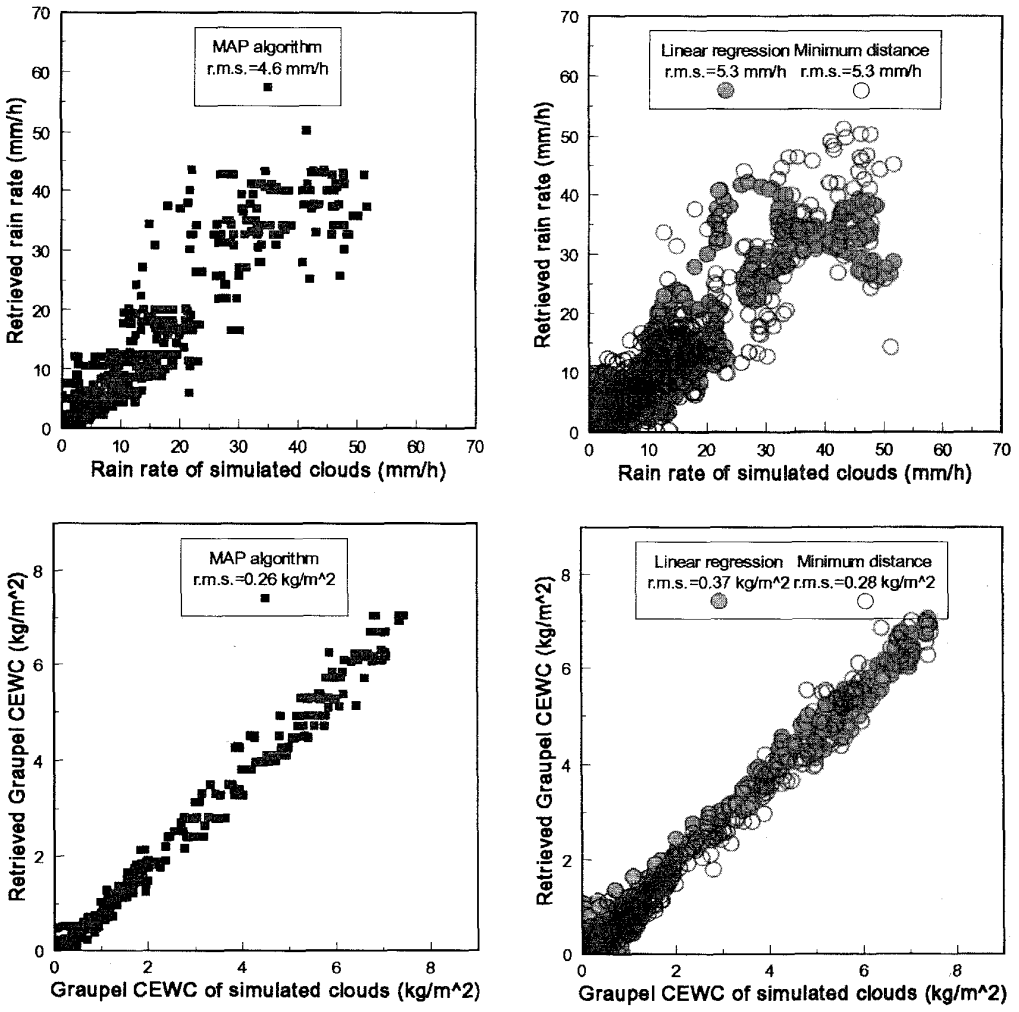

Fig. 9. Correlation diagrams between (top panels) rain rate and (bottom panels) graupel CEWC of test clouds and those retrieved by the (left panels) MAP algorithm and the (right panels) linear regression and minimum distance algorithms.

cold front which has already passed over Central Italy, and the existence of minor precipitating cells over the land, particularly in the area of the Tuscany region (about 43 North, 12 East) corresponding to the Arno river basin.

A. The Spectral Adequateness of the Cloud-Radiation Data Base

It is significant to analyze the adequateness of the *cloud-radiation data base* to comprise the SSM/I microwave spectral signature of the considered event. As an example, we consider the rainfall event in the Arno basin. Fig. 11 shows the comparison of the brightness temperatures measured by SSM/I in the precipitation area and the brightness temperatures of the *cloud-radiation data base* (the same points of Fig. 7 related to precipitation over land). The top panel of Fig. 11 compares the lowest frequency channels while the bottom panel presents the highest frequency channels. The adequateness can be considered fairly satisfactory, apart from a few image pixels. In particular, at the lowest frequencies the effect of the Earth's surface emissivity can be significant and probably requires a better modeling. It is important to point out that these results are obtained after the use of the deconvolution procedure, to make the ground resolutions of all microwave channels more comparable. In any case, the beam-filling effect on the spectral signature of SSM/I at the lowest frequencies should be assessed when doing these kind of comparison.

B. Results and Comparison with Raingauge Data

Comparisons between rain retrieval results obtained with the proposed algorithm and the raingauge measurements, always offer marked difficulties. Raingauge measurements often give cumulative values within one hour, so that they are time averaged, while T_B measurements on the contrary are spatially averaged. The raingauge networks, which one uses, are often installed for purposes other than those required for testing radiometric experiments. Their number in a given area is not always large enough to assume that more than one sensor is located in each SSM/I pixel and location errors in the

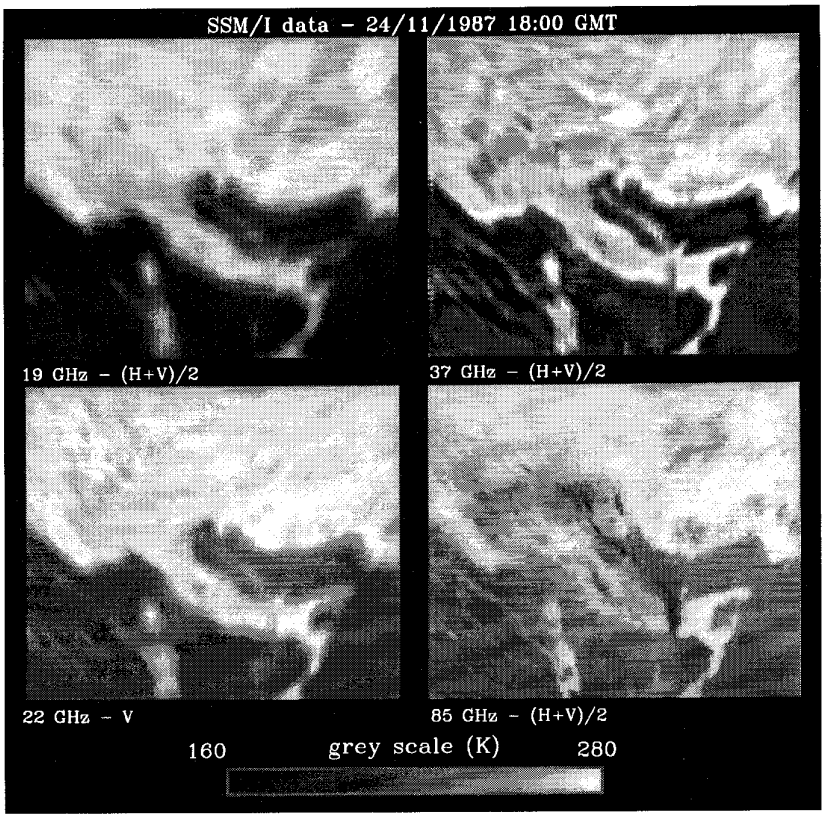

Fig. 10. Multifrequency image data acquired by SSM/I over the Mediterranean area at 18:00 GMT, during the Arno flood event (22 GHz vertically polarized data and 19, 37, and 85 GHz data averaged on the two polarizations).

radiometric images may cause problems when comparing the rain field pattern of a single precipitation event. However, some interesting comparison can be profitably made. We have chosen a test area in the Arno basin in Central Italy where a network of 16 raingauges already existed and the meteorological conditions during the satellite passage refer to a post cold front passage with few rainy cells left over and a fairly weak precipitation. Fig. 12 shows the surface rain rate map obtained by the retrieval procedure applied to the radiometric data of Fig. 11. The raingauge locations are also shown. In Table II we have reported separately the rain rate measured by the raingauges at 17:00, 18:00, and 19:00 GMT and estimated from the SSM/I pixel where at least one raingauge is present. It results that the average rain calculated from raingauges and from SSM/I data are, respectively, 2.2 and 1.8 mm/h. It should be noted that errors in the screening procedure and in the geolocation of the SSM/I pixels may have relevant effects when the rain pattern is remarkably nonhomogeneous as is the case of Fig. 12.

VII. Conclusion

In this paper, a method to infer precipitating cloud parameters from microwave radiometric data has been presented and tested on simulated data. The algorithm is essentially based on an extended and fairly dense data base of precipitating cloud structures and their related brightness temperatures. It uses a MAP criterion to select the most probable cloud given a multifrequency radiometric measurement. Hereafter, the main advantages of the proposed method are summarized.

- The simulation of the precipitating cloud structures accounts for the detailed information on hydrometeor profiles derived from a microphysical cloud mesoscale model.
- The consideration of the coarse hydrometeor profiles in addition to the surface rain rate allows one to take into account the vertical correlation between hydrometeors and to determine other quantities relevant in meteorological and hydrological processes.
- The use of a MAP criterion to determine the hydrometeor profiles allows one to properly account for instrumental and model errors and to incorporate different *a priori* information (e.g., the *a priori* probability of a class of precipitating events can be related to the geographical area of interest).
- Good performances in terms of computer time are achieved due to the adopted numerical implementation of the MAP criterion that searches the solution in the *cloud-radiation data base,* instead of operating in an iterative way.
- Tests on simulated data have proved that the rain rate estimation accuracy is improved in comparison to the linear regression and minimum distance algorithms.

Both potentials and drawbacks of the proposed method may together furnish guidelines for future developments, as indicated

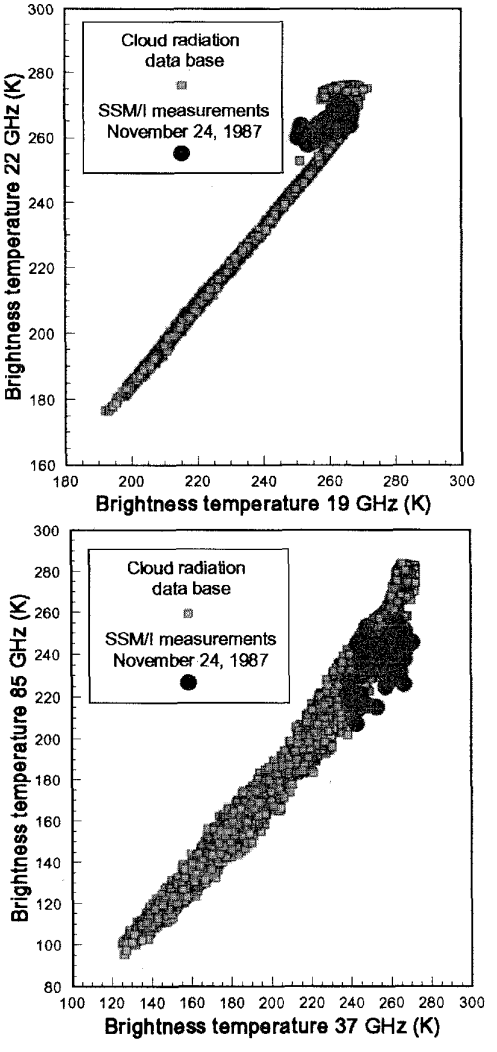

Fig. 11. Comparison of brightness temperature (T_B) values measured by SSM/I in the precipitation area with T_B values of the *cloud-radiation data base* (over land).

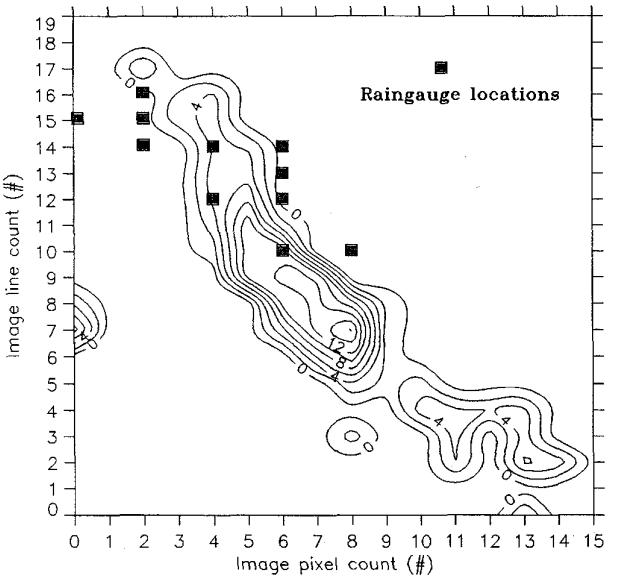

Fig. 12. Contour map of the surface rain rate retrieved from the SSM/I data shown in Fig. 11 and limited to the precipitation system over the Arno basin. The pixels where at least one raingauge measurement is located are indicated by a black square.

TABLE II
HOURLY CUMULATIVE RAIN RATE MEASURED BY THE RAINGAUGES AT 17:00, 18:00, AND 19:00 GMT AND INSTANTANEOUS RAIN RATE ESTIMATED AT 18:00 GMT FROM THE SSM/I PIXELS WHERE AT LEAST ONE RAINGAUGE IS PRESENT. THE SSM/I PIXEL AND LINE COUNTS REFER TO THE RAIN MAP OF FIG. 12

raingauges 17 GMT	raingauges 18 GMT	raingauges 19 GMT	SSM/I estimates	SSM/I pixel count	SSM/I line count
2.7	1.2	1.9	4.4	4	12
2.9	0.1	5.1	11.3	6	10
3.2	1.0	2.7	4.4	4	14
5.2	2.5	1.8	0	6	14
3.4	0.2	5.2	0	0	15
0.8	0.4	2.0	0	2	16
2.6	3	2.7	0	8	10
0.5	1.3	1.4	0	2	15
1.3	0	4.3	0	2	14
2.5	0.8	1.5	0	6	12
1.2	2.9	2.2	0	6	13

in the following points.

- The potential of the MAP criterion to account for more realistic assumptions about instrumental and model errors should be exploited; specifically, the dependence of the error on the frequency channel and the correlations between channels should be evaluated.
- The potential of the MAP criterion to account for *a priori* information about the probability of a class of precipitating events should be exploited and related to the geographical area of interest and time of the year in a routine processing of SSM/I data.
- The *extended cloud data base* should be upgraded to include meteorological conditions of different geographical regions and different types of precipitation events. This can be in principle accomplished by including in the procedure further outputs of microphysical models or radar data, or by slightly changing some statistical parameters of each identified class of clouds when required.
- The *cloud-radiation data base* should be consequently upgraded, including also some improvements of the radiative transfer model. In particular, the model assumption about the size distribution of particles and the hypothesis of horizontal homogeneity of the clouds should be critically revised.
- Besides some case studies using SSM/I data presented here and in previous papers, a systematic validation activity is required and is planned in the framework of international experiments (e.g., Algorithm Intercomparison Project, WetNet Precipitation Intercomparison Project).

REFERENCES

[1] E. C. Barrett and D. W. Martin, *The Use of Satellite Data in Rainfall Monitoring*. London: Academic, 1981.
[2] T. T. Wilheit, "Some comments on passive microwave measurement of rain," *Bull. Amer. Meteor. Soc.*, vol. 67, pp. 1226–1232, 1986.
[3] J. Simpson, R. F. Adler, and J. R. North, "A proposed Tropical Rainfall Measuring Mission (TRMM) satellite," *Bull. Amer. Meteor. Soc.*, vol. 69, pp. 278–295, 1988.

[4] A. Mugnai, E. A. Smith, and G. J. Tripoli, "Foundations for statistical-physical precipitation retrieval from passive microwave satellite measurements. Part II: Emission source and generalized weighting function properties of a time-dependent cloud-radiation model," *J. Appl. Meteor.*, vol. 32, no. 1, pp. 17–39, Jan. 1993.
[5] T. T. Wilheit, A. T. C. Chang, M. S. V. Rao, E. B. Rodgers, and J. S. Theon, "A satellite technique for quantitatively mapping rainfall rates over the ocean," *J. Appl. Meteor.*, vol. 16, pp. 551–560, 1977.
[6] K. S. C. Stamnes, S. C. Tsay, W. Wiscombe, and K. Jayaweera, "A numerically stable algorithm for discrete-ordinate-method radiative transfer in multiple scattering and emitting layered media," *Appl.Opt.*, vol. 27, no. 12, pp. 2502–2509, June 1988.
[7] P. Basili, P. Ciotti, G. d'Auria, F. S. Marzano, N. Pierdicca, and A. Mugnai, "A simulation study for retrieving rainfall from spaceborne microwave radiometers," in *Specialist Meeting on Microwave Radiometry and Remote Sensing Applications,* E. R. Westwater, Ed., Nat. Ocean. Atmos. Admin., Boulder, CO, June 1992, pp. 251–256.
[8] C. Kummerow, R. A. Mack, and I. M. Hakkarinen, "A self-consistency approach to improve microwave rainfall rate estimation from space," *J. Appl. Meteor.*, vol. 28, pp. 869–884, Sept. 1989.
[9] E. A. Smith and A. Mugnai, "Radiative transfer through a precipitating cloud at multiple microwave frequencies. Part II: Results and analysis," *J. Appl. Meteor.*, vol. 27, pp. 1074–1091, 1988.
[10] E. A. Smith, A. Mugnai, H. J. Cooper, G. J. Tripoli, and X. Xiang, "Foundations for statistical-physical precipitation retrieval from passive microwave satellite measurements. Part I: Brightness-temperature properties of a time-dependent cloud-radiation model," *J. Appl. Meteor.*, vol. 31, no. 6, pp. 506–531, June 1992.
[11] R. F. Adler, H. Y. M. Yeh, N. Prasad, W. K. Tao, and J. Simpson, "Microwave simulations of a tropical rainfall system with a three-dimensional cloud model," *J. Appl. Meteor.*, vol. 30, pp. 924–953, July 1991.
[12] P. Basili, P. Ciotti, G. d'Auria, F. S. Marzano, N. Pierdicca, and A. Mugnai, "Cloud microphysical model application to multivariate analysis of satellite microwave radiometric data," in *Specialist Meeting on Microwave Radiometry and Remote Sensing Applications,* E. R. Westwater, Ed., Nat. Ocean. Atmos. Admin., Boulder, CO, June 1992, pp. 245–249.
[13] P. Basili, P. Ciotti, G. d'Auria, F. S. Marzano, and N. Pierdicca, "A microwave radiometry characterization of precipitating clouds," in *Microwave Radiometry and Remote Sensing Applications,* D. Solimini, Ed. Utrecht, The Netherlands: VSP Int. Sci. Publ., 1995, pp. 229–237.
[14] C. D. Rodgers, "Retrieval of atmospheric temperature and composition from remote measurements of thermal radiation," *Rev. Geophys. Space Phys.*, vol. 14, no. 4, pp. 609–624, Nov. 1976.
[15] T. R. Wilheit, S. Adler, E. Barret, P. Bauer, W. Berg, A. Chang, J. Ferriday, N. Grody, S. Goodman, C. Kidd, D. Kniveton, C. Kummerow, A. Mugnai, W. Olson, G. Petty, A. Shibata, E. Smith, and R. Spencer, "Algorithms for the retrieval of rainfall from passive microwave measurements," *Remote Sensing Rev.*, vol. 11, pp. 163–194, 1994.
[16] E. A. Smith, X. Xiang, A. Mugnai, and G. J. Tripoli, "Design of an inversion-based precipitation profile retrieval algorithm using an explicit cloud model for initial guess microphysics," *Meteor. Atmos. Phys.*, vol. 54, pp. 1–28, 1994.
[17] A. J. Gasiewski and D. H. Staelin, "Statistical precipitation cell parameter estimation using passive 118-GHz O_2 observations", *J. Geophys. Res.*, vol. 94, no. D15, pp. 367–378, Dec. 1989.
[18] C. Prabhakara, G. Dalu, L. Liberti, J. J. Nucciarone, and R. Suhasini, "Rainfall estimation over oceans from SMMR and SSM/I microwave data," *J. Appl. Meteor.*, vol. 31, pp. 532–552, June 1992.
[19] F. S. Marzano, A. Mugnai, E. A. Smith, X. Xiang, J. Turk, J. Vivekanandan, "Active and passive microwave remote sensing of precipitating storms during CaPE. Part II: Intercomparison of precipitation retrievals over land from AMPR radiometer and CP-2 radar," *Meteor. Atmos. Phys.*, vol. 54, pp. 29–51, Mar. 1994.
[20] C. Kummerow and L. Giglio, "A passive microwave technique for estimating rainfall and vertical structure information from space. Part I: Algorithm description," *J. Appl. Meteor.*, vol. 33, pp. 3–18, Jan. 1994.
[21] P. Basili, P. Ciotti, F. S. Marzano, N. Pierdicca, and A. Albertone, "Precipitation Remote Sensing based on Spaceborne Multifrequency Microwave Radiometry," in *Proc. 6th Int. Symp. Physical Measurements and Signatures in Remote Sensing,* Val d'Isere, France, Jan. 17–21, 1994, pp. 458–467.
[22] K. F. Evans, J. Turk, T. Wong, and G. L. Stephens, "A Bayesian approach to microwave precipitation retrieval," *J. Appl. Meteor.*, vol. 34, no. 1, pp. 260–279, Jan. 1995.
[23] J. P. Hollinger, J. L. Peirce, and G. A. Poe, "SSM/I instrument evaluation," *IEEE Trans. Geosci. Remote Sensing* vol. 28, no. 5, pp. 781–790, Sept. 1990.
[24] M. R. Farrar and E. A. Smith, "Spatial resolution enhancement of terrestrial features using deconvolved SSM/I microwave brightness temperatures," *IEEE Trans. Geosci. Remote Sensing* vol. 30, no. 2, pp. 349–355, Mar. 1992.
[25] N. Grody, "Classification of snow cover and precipitation using the Special Sensor Microwave/Imager," *J. Geophys. Res.*, vol. 96, no. D4, pp. 7423–7435, Apr. 1991.
[26] R. W. Spencer, H. M. Goodman, and R. E. Hood, "Precipitation retrieval over land and ocean with SSM/I: Identification and characteristics of the scattering signal," *J. Atmos. Ocean. Tech.*, vol. 6, pp. 254–273, 1989.
[27] G. J. Tripoli, "A nonhydrostatic model designed to simulate scale interaction," *Mon. Wea. Rev.*, vol. 120, pp. 1342–1359, 1992.
[28] M. N. O. Sadiku, "Monte Carlo methods in an introductory Electromagnetic course," *IEEE Trans. Educ.*, vol. 33, no. 1, pp. 73–80, Feb. 1990.
[29] H. J. Liebe, "An updated model for millimeter propagation in moist air," *Radio Sci.*, vol. 20, no. 5, pp. 1069–1089, Sept.-Oct. 1995.
[30] W. Wiscombe, "Improved Mie scattering algorithm," *Appl. Opt.*, vol. 19, pp. 1505–1509, 1977.
[31] A. Mugnai and E. A. Smith, "Radiative transfer through a precipitating cloud at multiple microwave frequencies. Part I: Model description," *J. Appl. Meteor.*, vol. 27, pp. 1055–1077, 1988.
[32] F. S. Marzano, A. Mugnai, N. Pierdicca, E. A. Smith, J. Turk, and J. Vivekanandan, "Precipitation profile retrieval from airborne microwave radiometers: a case study over ocean during CaPE," in *Microwave Radiometry and Remote Sensing Applications,* D. Solimini, Ed. Utrecht, The Netherlands: VSP Int. Sci. Publ., 1995, pp. 253–263.
[33] L. Roberti, J. Haferman, and K. Kummerow, "Microwave radiative transfer through horizontally inhomogeneous precipitating clouds", *J. Geophys. Res.*, vol. 99, pp. 16707–16718, 1994.

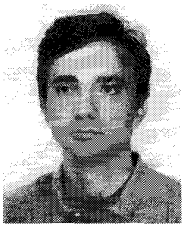

Nazzareno Pierdicca was born in Rome, Italy, on June 11, 1954. He received the Laurea (Doctor's) degree in electronic engineering (cum laude) from the University "La Sapienza," Rome, Italy, in 1981.

During 1978–1982, he was with the Italian Agency for Alternative Energy (ENEA) performing research and development activities in the field of thermal and mechanical behavior of the nuclear fuel rod. From 1982 to 1990, he worked with Telespazio, Rome, in the Remote Sensing Division. He was involved in various projects concerning remote sensing applications, data interpretation and ground segment design as responsible for the Instrument and Techniques branch of the Earth Observation Department. He was Principal Investigator of the ESA/JRC Agrisar '86 airborne campaign and Co-Investigator of the X-SAR/SIR-C experiment. In November 1990, he joined the Department of Electronic Engineering of "La Sapienza" University of Rome. His research activity mainly concerns electromagnetic scattering model, microwave radiometry of the atmosphere, SAR applications to vegetation. He is Investigator of the MAC Europe '91 and X-SAR/SIR-C experiments. He teaches Remote Sensing at the Faculty of Engineering of the University "La Sapienza" of Rome.

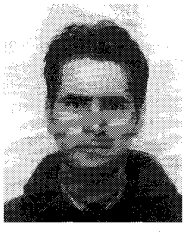

Frank Silvio Marzano received the Laurea degree (cum laude) in electrical engineering (1989) and the Ph.D. degree (1993) in applied electromagnetic from the University "La Sapienza," Rome, Italy.

Since then, he has been the recipient of a fellowship of the Italian Space Agency and, presently, he has a Postdoctoral position with the Department of Electronic Engineering of "La Sapienza," University of Rome. His current researches concern passive and active remote sensing of the atmosphere from airborne and spaceborne platforms, radiative transfer modeling of scattering media and scintillation analysis along satellite microwave links. He was involved in the Multi-Aircraft-Campaign (MAC Europe) in 1991, the Global Precipitation Climatology Project-Algorithm Intercomparison Projects (GCPC-AIP-2 in 1992 and GCPC-AIP-3 in 1995), and the WetNet Precipitation Intercomparison Project in 1994 (PIP-2).

Dr. Marzano received the Young Scientist Award of XXIV General Assembly of the International Union of Radio Science (URSI) in 1993.

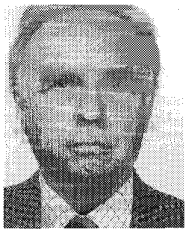

Giovanni d'Auria was born in Rome, Italy, on June 23, 1931. He obtained the degree in electrical engineering from the University "La Sapienza," Rome, Italy, in 1956 and the Libera Docenza degree in 1964, also from the same university.

He served in the Italian Air Force, working in ITAV Laboratories. He was then with Fondazione Ugo Bordoni as Researcher in the Antennas and Propagation Laboratory. He joined the Department of Electronics, University of Rome, in 1962 as an Assistant Professor, teaching applied electronics. In 1976 he was appointed Professor in the Chair of Antennas and Propagation and has been teaching this subject ever since. His current research concerns EM propagation in a turbulent atmosphere, microwave remote sensing of the atmosphere and Earth's surface, microwave radiometry of the atmosphere, and particularly of cloud systems.

Dr. d'Auria is currently an official member of Comm. F of the Italian Committee of URSI.

Patrizia Basili was born in Rome, Italy, on March 17, 1947. She graduated in electrical engineering from the University of Rome, Rome, Italy, in 1972.

In 1973 she joined the Department of Electrical Engineering of the University of Rome were she taught courses on electromagnetic fields. She is now Full Professor at the Institute of Electronics, University of Perugia, Perugia, and teaches a course on remote sensing. She has also taught courses on electromagnetic wave theory (Calabria University, 1977) and antennas and propagation (Ancona University, 1978–1980). Her research activity has been concerned with microwave and millimiter-wave propagation in the atmosphere, atmospheric remote sensing by radiometry, and inverse problems in electromagnetics.

Piero Ciotti (M'94) was born in Rome, Italy, on November 10, 1952. He received the degree in electrical engineering (cum laude) from the University of Rome, Italy, in 1977.

He joined the Department of Electrical Engineering of the University of Rome in 1977 where he served first as an Assistant Professor and, since 1987, as an Associate Professor, teaching a course on remote sensing. During 1984–1985, he conducted research at the NOAA/ERL Wave Propagation Laboratory, Boulder, CO, on a NATO/CNR fellowship. Since 1991 he has been with the Department of Electrical Engineering of the University of L'Aquila, L'Aquila, Italy, where he has taught courses on signal theory (since 1991), electromagnetic fields (since 1992), and electromagnetic wave propagation (since 1994). His research activity has been concerned with radiometric remote sensing of the atmosphere, microwave line-of-sight propagation, inverse electromagnetic problems, and digital signal processing.

Alberto Mugnai received the Laurea (cum laude) degree in physics from the University of Florence, Italy.

He is presently the Director of the Institute of Atmospheric Physics (IFA) of the National Research Council (CNR). His current researches concern microwave radiative transfer in clouds, nowcasting, and satellite meteorology. He is Associate Editor of the *Journal of the Atmospheric Sciences*, member of the Precipitation Mission Working Group of the European Space Agency (ESA), member of the Science Advisory Group for the Multifrequency Imaging Microwave Radiometer (MIMR) of ESA, and Principal Investigator of the WetNet Project of the National Aeronautics and Space Administration (NASA).